


Transient chaos and memory effect in the Rosenzweig-MacArthur system with dynamics of consumption rates

Przemysław Gawroński¹, Jarosław Kwapien², and Krzysztof Kułakowski¹

¹*Faculty of Physics and Applied Computer Science, AGH University of Krakow, al. Mickiewicza 30, PL-30059 Kraków, Poland*

²*Institute of Nuclear Physics, Polish Academy of Sciences, ul. Radzikowskiego 152, PL-31342 Kraków, Poland*

 (Received 10 August 2023; revised 29 January 2024; accepted 20 February 2024; published 18 March 2024)

We consider the system of the Rosenzweig-MacArthur equations with one consumer and two resources. Recently, the model has been generalized by including an optimization of the consumption rates β_i [P. Gawroński *et al.*, *Chaos* **32**, 093121 (2022)]. Also, we have assumed that $\beta_1 + \beta_2 = 1$, which reflects the limited amount of time that can be devoted to a given type of resource. Here we investigate the transition to the phase where one of the resources becomes extinct. The goal is to show that the stability of the phase with two resources strongly depends on the initial value of β_i . Our second goal is to demonstrate signatures of transient chaos in the time evolution.

DOI: [10.1103/PhysRevE.109.034210](https://doi.org/10.1103/PhysRevE.109.034210)

I. INTRODUCTION

Population dynamics is a cornerstone of theoretical ecology [1–3], with links to economic sciences [4] and game theory [5], and with the Lotka-Volterra [6,7] and Rosenzweig-MacArthur (RMA) [8] models as leading examples. The latter approach has been advanced in recent years on a variety of fronts. The tools applied include fractional derivatives [9], time discretization [10], and stability analysis [11], among others. Often the objective is to capture a given phenomenon, such as paradox of enrichment [12], variable mortality [13], prey taxis [14], spatial distribution of population [15], nonlinear diffusion [16], traveling waves [17], hydra effect [18], chimera patterns [19], synchrony and asynchrony [20], and others. Taking into account a spatial dependence [15,21] of the density of consumers and/or resources (predators and prey) allows considering various means of hunting and/or escape [22,23]. Although certainly incomplete, this list places the RMA model at the core of modeling ecological systems.

The concept of dynamic optimization appears here in a natural way as an ongoing modification of decision variables to improve consumption [24,25]. This can be achieved by allowing the variables to depend on the current state of the system. Optimization of this kind of predator search rate has been implemented for a model of one consumer and one resource [26], and it was shown to convert the functional response from the Holling II to Holling III type. Another form of dynamic optimization is to impose the condition of maximal consumption, at each point of the trajectory, by appropriate values of the decision variables. Then, the states with maximal consumption are reached immediately. This approach has been applied in a series of papers by Křivan *et al.* [27–29].

In our recent article [30], a dynamic optimization of the consumption rates of two resources by a consumer has been discussed within the RMA model for one consumer and two resources. The dynamic character of the rates β_i has been implemented via an additional equation of motion of the rates, $d\beta_i/dt = v\partial C/\partial\beta_i$, where C is the density of the consumer, the consumption rates of the resources R_i are bound by the

condition $\beta_1 + \beta_2 = 1$, and v is a parameter. The evolution $d\beta_i/dt$ is equivalent to an application of one step of the gradient ascent method. In this way, and contrary to Ref. [29], the model has a tendency to optimize with speed controlled here by the factor v . In this way, the dynamic optimization in our approach can be treated as an intermediate solution between the static optimization where the consumption rates are constant and the solution where the consumption is maximized immediately in each time step. The former technique has already been announced in *Foraging Theory* by Stephens and Krebs ([24], p. 151). The latter has been worked out by Křivan *et al.* [29]. Effectively, in our formulation the velocity of optimization is positive and finite. On the other hand, dynamic optimization as such can be seen as a gradual approach to equilibrium in game-theoretical problems, as duopolies of various kinds. We believe that our assumption of gradual variation of the rates β_i is more realistic than the case of static optimization, where the rates do not change, and than immediate optimization (as in Ref. [29]).

In Ref. [30], a phase diagram has been worked out in a plane (α_{ii}, v) , where α_{ii} is a Verhulst-like coefficient in the time evolution of the i th resource. There, two phases have been identified, say B and G, which differ in the number of active (nonzero) resources: two resources in phase B and only one in phase G. The aim of the present paper is to explore the system dynamics: When and how does the transition from B to G appear?

In the present paper, our goals are as follows. First, a chaotic behavior is identified at the early stage of the time evolution. Second, it is shown that the stationary phase diagram of the system preserves memory of the initial values of the rates β_i ; in particular, the critical value of the parameter v where the transition from phase B to phase G is strongly dependent on $\beta_i(t=0)$.

In the next section, the model equations are given, together with values of these parameters, which remain fixed throughout the text. Section III is devoted to the numerical results: the temporally chaotic character of the solutions (the

so-called transient chaos [31,32]) and the dependence of the phase diagram on the initial values of the rates β_i . The results are discussed in the last section.

II. THE MODEL

In the RMA model, the equations of motion for the densities of consumer C and two resources R_i , $i = 1, 2$ are [33]

$$\frac{dC}{dt} = pC \frac{\beta_1 R_1 + \beta_2 R_2}{1 + b(\beta_1 R_1 + \beta_2 R_2)} - mC, \quad (1)$$

$$\frac{dR_1}{dt} = R_1(1 - \alpha_{11}R_1 - \alpha_{12}R_2) - \frac{pR_1\beta_1 C}{1 + b(\beta_1 R_1 + \beta_2 R_2)}, \quad (2)$$

$$\frac{dR_2}{dt} = R_2(1 - \alpha_{21}R_1 - \alpha_{22}R_2) - \frac{pR_2\beta_2 C}{1 + b(\beta_1 R_1 + \beta_2 R_2)}, \quad (3)$$

where β_i is the rate of taking advantage of resource R_i , and α_{ij} is the Verhulst term which produces a limitation of growth of resource R_i , imposed by resource R_j . Further, p is the attack rate of the consumer, b is the Holling's II functional response term of the consumer, and m is the mortality rate of the consumer [33].

As in Ref. [30], these equations are supplemented as follows. The first is the condition $\beta_1 + \beta_2 = 1$, which denotes a limitation of time of the consumer devoted to a given resource. This limitation can be seen as a simple example of "an interaction between interactions" [34]; namely, the active consumption of one resource hampers the consumption of another one.

Further, the rates β_i are also subject to time evolution, according to the rule

$$\frac{d\beta_i}{dt} = v \frac{\partial C}{\partial \beta_i}, \quad (4)$$

where $i = 1, 2$, the right-hand side derivative is of the function $C(\beta_1, \beta_2) = C(\beta_1, 1 - \beta_1)$ for $i = 1$, $C(\beta_1, \beta_2) = C(1 - \beta_2, \beta_2)$ for $i = 2$, and $1/v$ is the characteristic time of this evolution. In Eq. (4), we presuppose that β_1 is modified so as to enhance the consumer density C , and that the evolution speed is proportional to the yielded gain in C .

The values of some parameters are kept the same as in Ref. [30]: $\alpha_{12} = \alpha_{21} = 0.065$, $m = 0.2$, $p = 3.0$, $b = 2.0$ and $\alpha_{11} = \alpha_{22}$. For one consumer and one resource, where one of the β 's is zero, these values of p , m , and b produce limit cycles, with a Hopf bifurcation at $m = 0.5$. For two resources, the model is more complex. Below, we demonstrate that the stationary outcome of Eqs. (1)–(4) do depend on the initial conditions of the coefficients β_i .

III. RESULTS

As demonstrated in Ref. [30], the numerical solutions of Eqs. (1)–(4) for small v and asymptotically long times are composed of two modes, following each other. One mode is a variation of the four variables: C , R_1 , R_2 , and β_1 approximately linear in time. Another mode is their oscillation with a given frequency and amplitudes, which raise, next decrease. This behavior can be seen as two subsequent supercritical Hopf bifurcations in four-dimensional space. As the evolution is periodic in time, the solution can be identified as a homoclinic orbit. A similar sequence of burstlike modes has

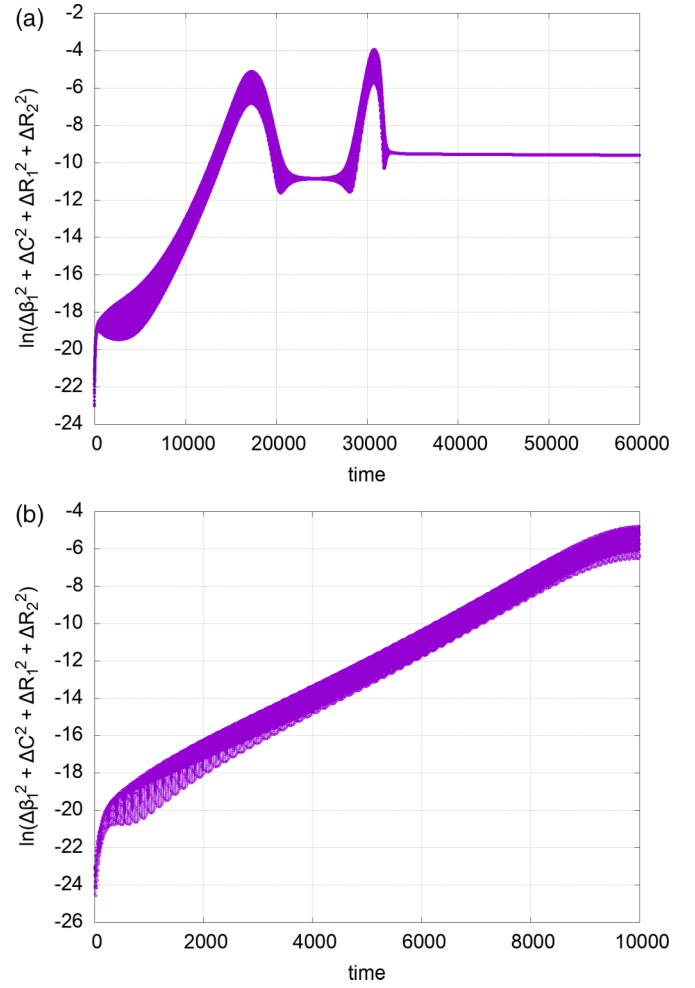


FIG. 1. (a) The time dependence of a squared distance between two initially close trajectories in the four-dimensional space C, R_1, R_2, β_1 . (b) The time dependence of a squared distance between two initially close trajectories; the time range is chosen to show the approximately exponential increase in time. (Parameters: $\alpha_{ii} = 0.80$, $v = 0.011300$, $\beta_1 = 0.53$).

been identified for the RMA model of a tritrophic system of a prey, a predator, and a superpredator [35]. There, both regular and chaotic behavior have been allowed. Irregular variations of trajectories with time are also observed here in the early stage of the simulation. Then we made an attempt to check the possible chaotic character of our solution.

First, we simulate the time dependence of a distance between two trajectories, initially close to each other. These results are shown in Figs. 1(a) and 1(b) for one turn of the homoclinic orbit. The apparent thickness of the plots comes from the fact that both compared trajectories oscillate. Indeed, there is some range of time where the plot on the logarithmic scale of the vertical axis is approximately linear, as shown in Fig. 1(b). The local slope, fitted within this range, is small yet positive.

However, as was argued in Ref. [31], this positive slope could just mean that the trajectory leaves some unstable region of phase space. As an additional criterion of the transient chaos, we measure the lifetime of the initial phase B when the system starts near the boundary between phases B and G,

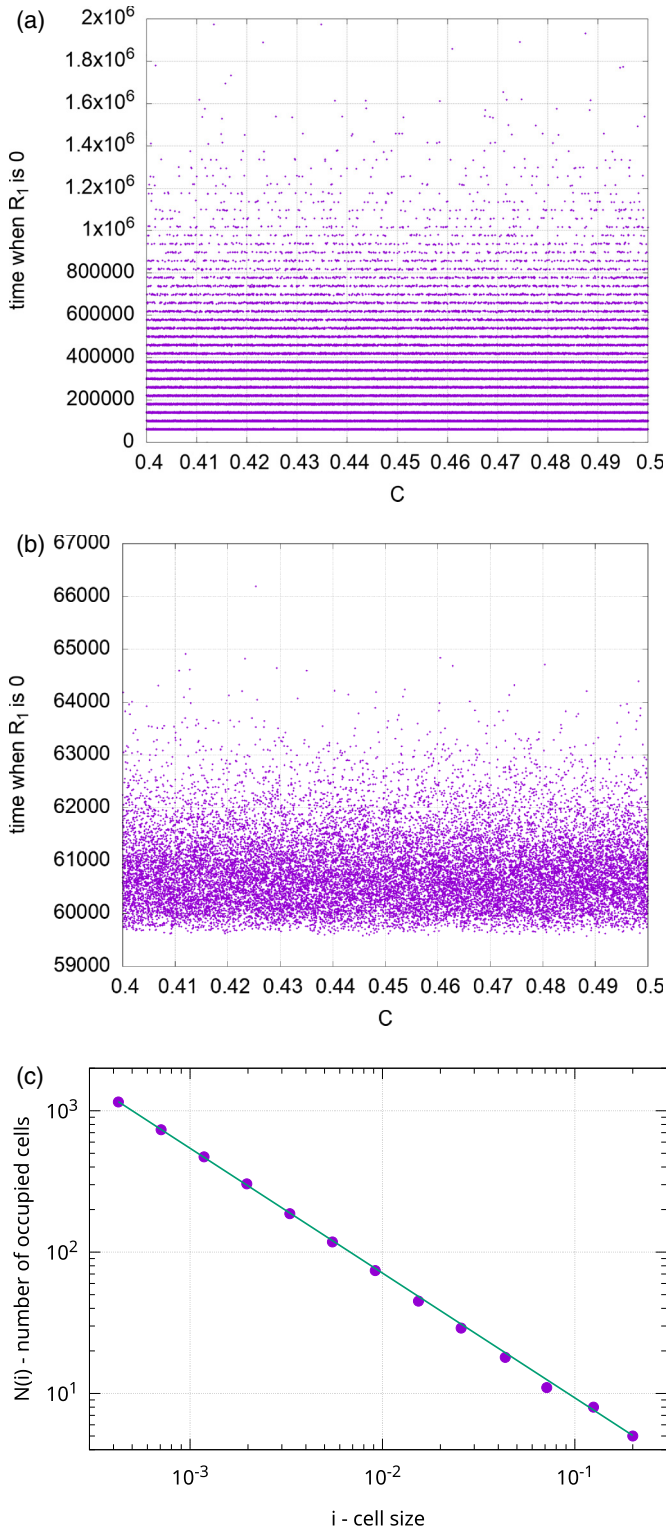


FIG. 2. (a) Time to obtain phase G dependent on the initial value of the consumer density, $C(t = 0)$. (b) Here only the lowest band is shown. The parameter v is slightly larger (by 0.022) than its critical value. (c) Fractal dimension ($D = 0.88$) of Fig. 2(b) calculated using the box counting method. (Parameters: $\alpha_{ii} = 0.96$, $v = 0.16$, $\beta_1 = 0.53$).

on the side where $v > v_{cr}$. (Recall that, above v_{cr} , the system ends in phase G.) The lifetime is measured as dependent on the initial conditions [31]; here we slightly change the initial

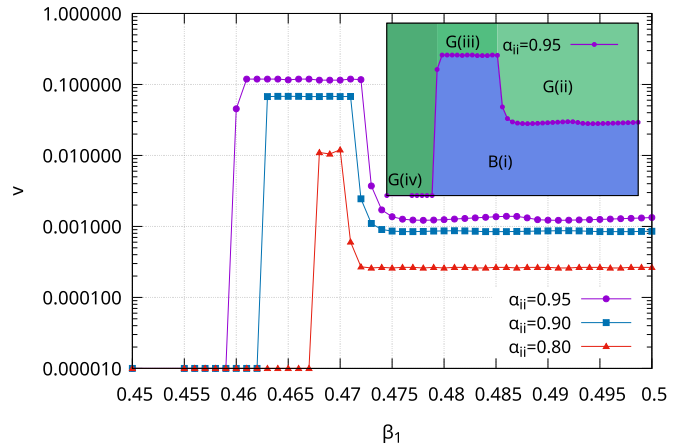


FIG. 3. Dependence of v_{cr} on $\beta_1(t = 0)$ for various α_{ii} . For $v > v_{cr}$, phase G appears. Below this line the system ends in phase B.

value of the consumer density C . The results are shown in Fig. 2. They indicate that the dependence is not a smooth curve, and suggest a fine—possibly fractal—structure of regions of phase space which lead to a given lifetime of phase B. To clarify this issue, an evaluation of the box-counting fractal dimension D of the data on the time of phase change, as dependent on the initial value of the consumer density. We note that these data show a characteristic time, related to the periodic behavior of R_i [visible also in Fig. 4(a)]; the transition to phase G where $R_i = 0$ occurs when R_i is of low value. This periodicity appears after the (transient) chaotic stage ends, and it produces the set of horizontal bands. Therefore, it makes sense to calculate the fractal dimension for one such band, shown in Fig. 2(b). The result is $D = 0.88$ (Fig. 2(c)), which confirms the fractal character of the data. [For completeness, we add that for the data shown in Fig. 2(a), the fractal dimension is found to be 0.68.]

To explore the influence of $\beta_1(t = 0)$ in its range wider than in Ref. [30], calculations of the boundary v_c between phases B and G are performed for the initial values of β_1 below 0.49. As we show in Fig. 3, there the dependence of v_c on $\beta_1(t = 0)$ is quite strong, namely, once the chaotic stage ends, either the system remains in phase B, where permanent oscillations are present, or the system tends to phase G, where one of the resources disappears. The latter transformation can appear either directly from the chaotic stage or from the periodic phase. Phase G is absorbing, which means that the transition to this phase is irreversible. In summary, one can distinguish four scenarios:

- (i) the system remains in phase B, where the variables oscillate,
- (ii) the system switches to phase G right from the chaotic phase,
- (iii) the system switches to phase G from the periodic phase, and
- (iv) the system starts from phase G.

Case (i) appears if the parameter v is smaller than its critical value. The following numbers apply to the case $\alpha_{ii} = 0.95$. Case (ii) appears if $0.475 < \beta_1(t = 0) < 0.525$. The critical value v_c of the parameter v is moderate, around 10^{-3} . Case

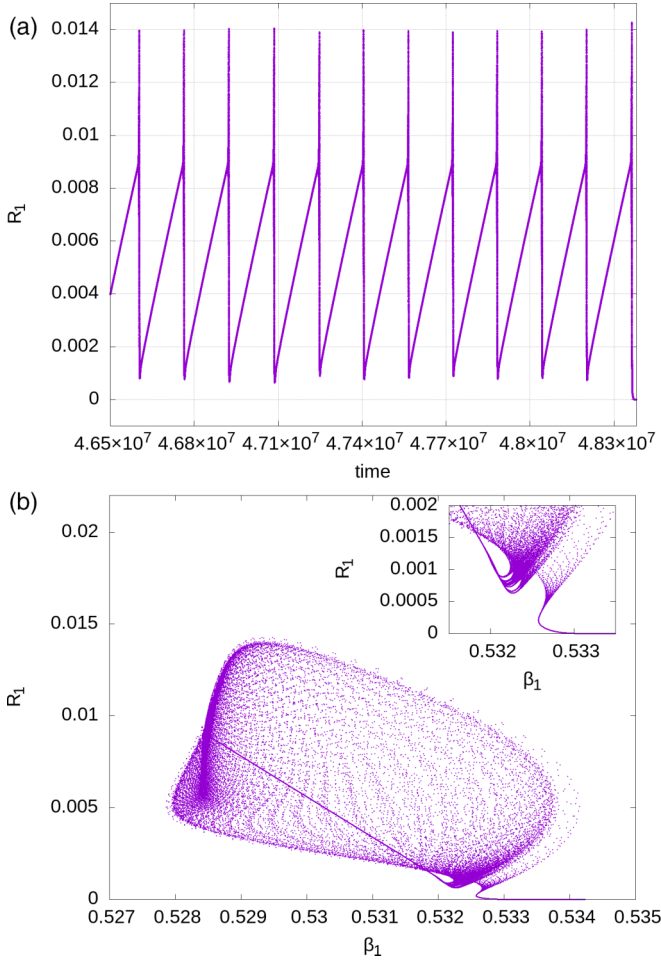


FIG. 4. Dependence of R_1 on (a) time and (b) β_1 : 12 last turns before switching to phase G. Inset. During the last turn the amplitude of the variation of β_1 is larger and the resource R_1 drops to zero. (Parameters: $\alpha_{ii} = 0.80$, $v = 0.011100$, $\beta_1 = 0.53$).

(iii) appears if $0.46 < \beta_1(t = 0) < 0.475$ or $0.525 < \beta_1(t = 0) < 0.54$. There, phase B is much more stable: v_c is about 0.1. Case (iv) appears if $|\beta_1(t = 0) - 0.5| > 0.04$. As seen in Fig. 3, for α_{ii} lower than 0.95 the behavior is qualitatively the same; it is only that the range of $\beta_1(t = 0)$ where case (iii) applies is narrower. In the inset of Fig. 3, a diagram is shown where cases (i)–(iv) have their counterparts as colored areas in the plane $[\beta_1(t = 0), v]$.

It is remarkable that a small variation of β_1 can lead to a huge change in the critical value v_c . To elucidate this point, we show in Figs. 4 and 5 examples of two modes of the transition. In Fig. 4, a part of the periodic trajectory $R_2(t)$ is shown, accompanied by projection to the plane (β_1, R_2) , just before its collision with the absorbing subspace $R_2 = 0$. This should be compared with Fig. 5, where the analogous trajectory is shown just before its collision with $R_2 = 0$ right from the chaotic stage. It is clear that the appearance of this collision strongly depends on the distance between the trajectory and its target $R_2 = 0$. Hence, a small change in the parameters can produce a large variation in the critical value of v_c . Accordingly, the large drop in v_c above $\beta_1(t = 0) = 0.47$ is due to the fact that in this range the transition to phase G appears directly from the transient stage (Fig. 5), while below this

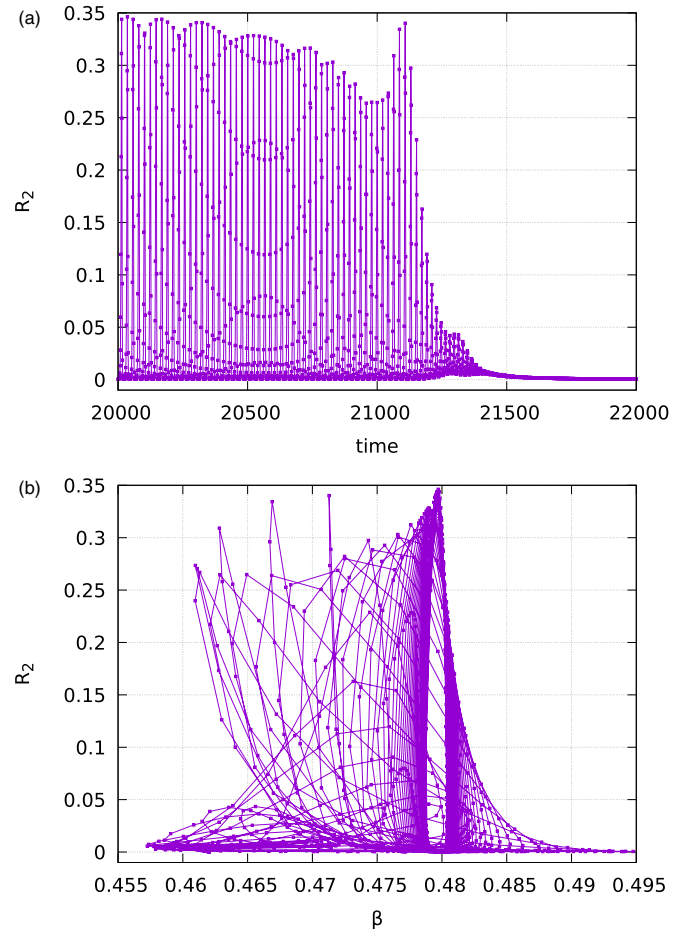


FIG. 5. Dependence of R_2 on (a) time and (b) β_1 at the transition to phase G, where $R_2 = 0$. (Parameters: $\alpha_{ii} = 0.90$, $v = 0.000865$, $\beta_1 = 0.49$).

range the transition is from the periodic stage of phase B, as shown in Fig. 4. The mechanism of the strong dependence of v_c on $\beta_1(t = 0)$ emerges as follows: either the crossover to phase G occurs earlier than the end of the transient chaotic behavior or not. In the former case, the time dependence of R_2 is more volatile, and the transition is easier. Otherwise, once the periodic (nonchaotic) behavior is achieved, the transition to phase G demands a much larger value of the parameter v .

To trace how the initial value of β_1 influences the system formed after the transient stage, two further calculations are performed. First, the Fourier spectrum of $R_2(t)$ is found for the stationary periodic state for phase B (v below v_c). As we show in Fig. 6, this spectrum is the same for all the investigated values of $\beta_1(t = 0)$. In other words, the initial value of β_1 does not influence the frequencies of $R_2(t)$. Second, we compare the trajectories of $\beta_1(t)$, $C(t)$, $R_1(t)$, and $R_2(t)$, starting from the same initial values of C , R_1 , and R_2 . Only $\beta_1(t = 0)$ was different: 0.47 for one trajectory and 0.48 for another. In Figs. 7 and 8, the differences are shown: $\Delta\beta_1(t)$ and $\Delta R_2(t)$ in the stationary state. The parameter v is taken as 0.001240, that is, just below its critical value 0.001245 for $\beta_1(t = 0) = 0.48$. As we see, the differences between the two trajectories are visible and never vanish in the stationary state for both $\Delta\beta_1(t)$ and $\Delta R_2(t)$. Additionally, the same effect is shown in Fig. 9. As we can see there, the time variation of $\Delta R_2(t)$ depends

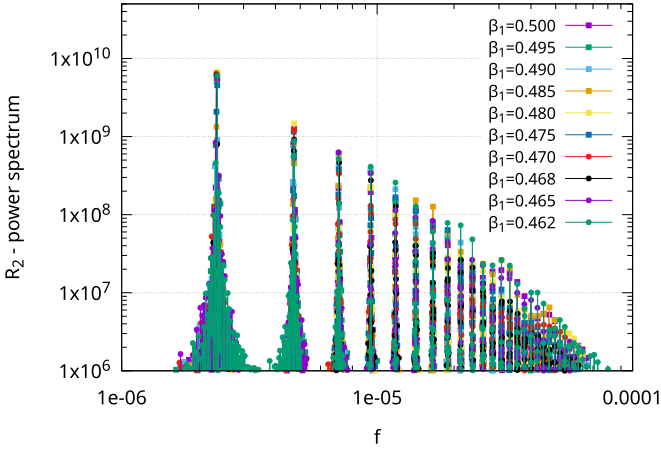


FIG. 6. Power spectrum of R_2 for various β_1 . Besides the original frequency f , the spectrum contains frequencies $2f$, $3f$, $4f$, etc. (Parameters: $\alpha_{ii} = 0.95$, $v = 0.001220$).

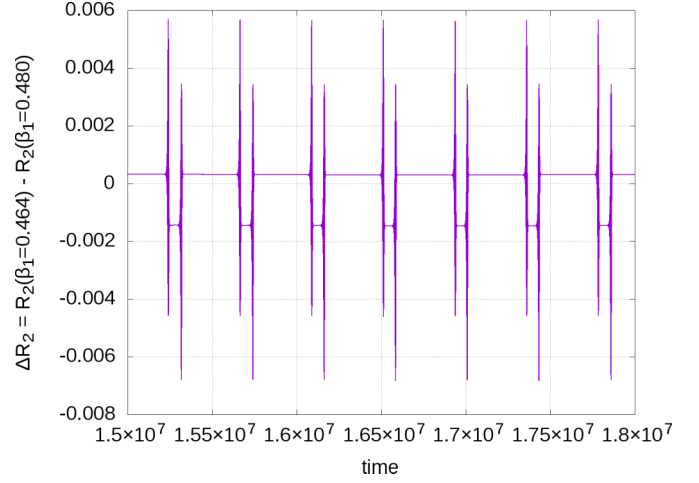


FIG. 9. Evolution of ΔR_2 for two initial values of $\beta_1 = 0.464$ and $\beta_1 = 0.48$, $\alpha_{ii} = 0.95$, $v = 0.001240$.

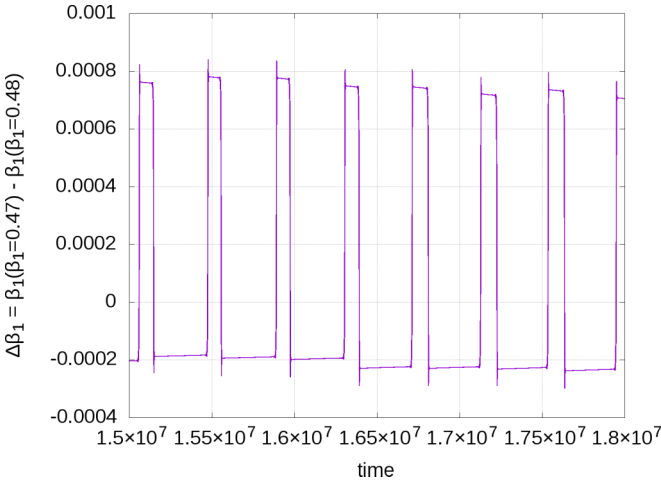


FIG. 7. Evolution of $\Delta\beta$ for two initial values of $\beta_1 = 0.47$ and $\beta_1 = 0.48$, $\alpha_{ii} = 0.95$, $v = 0.001240$.

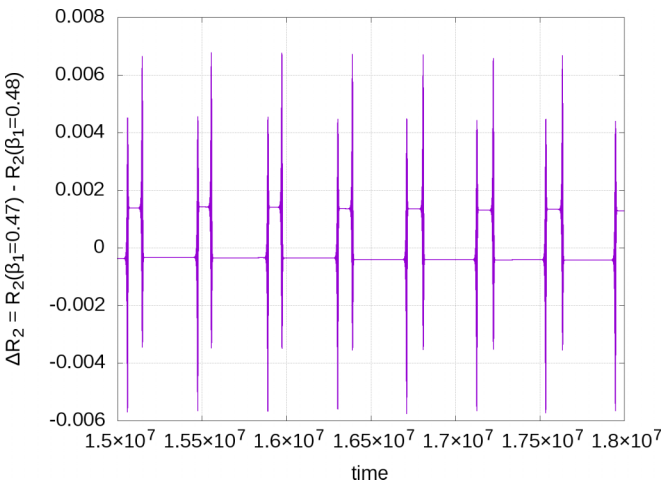


FIG. 8. Evolution of ΔR_2 for two initial values of $\beta_1 = 0.47$ and $\beta_1 = 0.48$, $\alpha_{ii} = 0.95$, $v = 0.001240$.

on the initial value of $\beta_1(t = 0)$, namely, a slight phase shift of the oscillations is observed between the two compared trajectories. Concluding, since the information about the initial values of the rates β_i appears to be preserved during the time evolution, we can speak about a memory effect.

We would like to add a note on the dependence of the boundary v_c between phases B and G on the coefficient α_{ii} , as reported in Ref. [30]. This boundary has been found to increase approximately linearly with α_{ii} to about $\alpha_{ii} = 0.96$, with an additional enhancement above this value. This result has been obtained for the initial values of the rates β_i equal to 0.49 and 0.5. The shape of the boundary v_c in the phase diagram can be qualitatively interpreted based on the analytical solution of Eqs. (1)–(3), for $v = 0$. Phase B stability analysis has been performed in Ref. [30]. It has been shown in Fig. 3 that there are two stable regions in the phase space, around $\beta_1 = 0.47$ and $\beta_1 = 0.53$. When analyzing the stability of phase G (for $v = 0$, $\beta_1 < 0.5$, and $R_2 = 0$), we get $R_1 = m/((p - mb)\beta_1)$ and $C = (1 - \alpha_{11}R_1)/((p - mb)\beta_1)$. There, two Jacobian eigenvalues are always negative and the third eigenvalue is equal to $1 - \alpha_{21}R_1 - pC\beta_2/(1 + b\beta_1R_1)$. This eigenvalue changes signs at some β_1^* ; it is negative for $\beta_1 < \beta_1^*$, which means that phase G is stable there. The value of β_1^* slowly decreases with α_{11} from 0.467 for $\alpha_{11} = 0.8$ to 0.457 for $\alpha_{11} = 0.99$. In other words, when α_{11} increases, the boundary of the stability area of phase G moves away from the boundary of the stability area of phase B (β_1 about 0.47 [30]). When these boundaries are more apart, phase B is more stable and v_c increases.

IV. DISCUSSION

From an experimental point of view, our results indicate a partial resilience of the system with respect to the optimization of consumer rates β_i . However, once the incentive (represented here as v) to change the phase is sufficiently strong, the system is converted to a different phase of lower diversity. These results add to a general belief in instabilities of ecological systems, a classic theme since the papers of Holling in the 70's [36], and provide an example of such a phase transition.

The main innovation of the original RMA model presented in Ref. [30] and here is that the consumption rates are controlled by the consumer to enhance its own density C . For this purpose, the rates β_i can evolve over time. Our model results indicate that once one of two resources happens to be exploited more clearly than another, this exploited resource is going to extinct. In contrast to the stochastic version of the so-called paradox of enrichment [12,37], otherwise similar, this extinction is deterministic, i.e., it will happen for sure in some definite subspace of the values of the parameters. (See also the discussion of the so-called atto-fox effect in Ref. [2]). At the end, that is, in the stationary state of phase G, C is indeed the largest. Simultaneously, the rate of consumption of the remaining resource is stabilized at a moderate value. On the other hand, the diversity of resources is lost. The literature on vanishing and endangered species is abundant [38], with overfishing as a particularly well-described phenomenon [39]. Our considerations here are limited to the model results; however, analogies impose easily.

It is tempting to consider the system of Eqs. (1)–(4) as an example of slow-fast model [40], with the dynamics of β_i 's slower than the dynamics of C, R_1, R_2 . In such considerations, the velocity v could play the role of a small parameter. However, the frequency of oscillations during the bursts is the same for all four variables, which makes the analogy doubtful. On the other hand, the case of $v = 0$ allows for qualitative insight into the observed phenomena observed numerically for $v > 0$. It is worthwhile to note that the strong effect of extinction of one resource is a consequence of a collision of boundaries of areas of stability of two phases, with only tiny motion of these boundaries. This aspect of our results brings attention to nonlinear answers of the environment to small changes of the imposed conditions.

The results add to several concepts related to theoretical ecology, making their definitions slightly wider. In Ref. [41], a kind of memory effect in the RMA model has been implemented with fractional derivatives. There, the time evolution of a function depends on its shape in the past. In contrast, here an actual phase related to a point (α_{ii}, v) in the phase diagram appears to depend on the initial values of β_i . Once phase B or G is given, the consumer density C has a well-defined value.

Another related concept is predator interference. As defined in Ref. [42], it is “a decline in the per predator consumption rate as predator density increases.” While other definitions [43,44] refer to more than one predator, the sentence above [42] suggests its applicability to our case. And, indeed, here the density of consumers is larger in phase G than in phase B, while the consumption rate β_i related to the nonvanishing resource R_i is clearly lower than the other $\beta_{3-i} = 1 - \beta_i$.

There is also some correspondence between the concept of control in the RMA model described in Ref. [45], and a

possible application of such control in our case. In Ref. [45] and references therein, a discrete-time scheme has been proposed for one consumer and one resource. To preserve nonzero values of the related variables, the so-called threshold policy with hysteresis has been applied, i.e., appropriate terms have been added to the model equations. It is straightforward to imagine a similar supplement of our equations of motion, which could maintain the evolution of the rates β_i in the range around 0.5. Such a supplement would be a direct generalization of the approach in Ref. [45] to the case of one consumer and two resources, which is worked out here.

The qualitative aspects of our results can be summarized as follows. First, the time evolution in the stationary state preserves information on the initial values of the rates β_i of consumption. Second, this information persists despite the (transient) chaotic episode at the beginning of the evolution. Third, the dependence of the critical velocity v_c on the initial value of rate β_1 is practically composed of three plateaus of clearly different values. These qualitative aspects of our results make the RMA system attractive for modeling economic and social systems. There, several approaches [46–48] are still based on the Lotka-Volterra model, despite its obvious shortcomings: the unbounded increase of preys in the absence of predators, and the constant of motion of periodic orbits, which leads to the atto-fox effect [2]. These shortcomings are removed when the so-called Verhulst term [49] is added; yet the RMA model allows us to also include the Holling functional response of type II, with a clear interpretation of overfeeding. There and in other papers [46–48], applications of the RMA model could be a step forward.

Abstracting from the details, our results indicate that after some transient chaotic stage, the system of a consumer and resources either oscillates in a predictable way or gets to a state where one of the resources is irreversibly extinct. Actually, research on a system of one consumer and two resources can only give some notions about complex trophic levels and food chains. Yet, transient chaos is also known to appear for larger systems [50]. From our considerations, two such notions can be drawn. The first is that complex networks of consumer-resource relations can persist if their evolutions in time are coherent, i.e., their oscillations in time self-organize to some common frequencies. This result is consistent with the discussion in Ref. [51]. Such oscillations, if not too large, can even stabilize the whole system [52]. The second is that a larger modification of a single variable can lead to a destabilization of a large part of the system, with the biological diversity reduced. This result adds to the general conclusions of Ref. [53].

ACKNOWLEDGMENT

The authors are grateful to A. Borzì and our anonymous referees for their insightful comments.

- [1] *Theoretical Ecology: Principles and Applications*, edited by R. May and A. R. McLean (Oxford University Press, New York, 2007).
 [2] C. Lobry, *The Consumer-Resource Relationship: Mathematical Modeling* (Wiley-ISTE, London, 2018).

- [3] *Theoretical Ecology: Concepts and Applications*, edited by K. S. McCann and G. Gellner (Oxford University Press, Oxford, 2020).
 [4] I. Almudi, F. Fatas-Villafranca, J. Palacio, and J. Sanchez-Choliz, Pricing routines and industrial dynamics, *J. Evol. Econ.* **30**, 705 (2020).

- [5] K. Grunert, H. Holden, E. R. Jakobsen, and N. Chr. Stenseth, Evolutionarily stable strategies in stable and periodically fluctuating populations: The Rosenzweig–MacArthur predator–prey model, *Proc. Natl. Acad. Sci. USA* **118**, e2017463118 (2021).
- [6] A. J. Lotka, *Elements of Physical Biology* (Williams and Wilkins, Baltimore, 1925).
- [7] V. Volterra, Variations and fluctuations of the number of individuals in animal species living together, *ICES J. Mar. Sci.* **3**, 3 (1928).
- [8] M. L. Rosenzweig and L. H. MacArthur, Graphical representation and stability conditions of predator-prey interactions, *Am. Nat.* **97**, 209 (1963).
- [9] H. S. Panigoro, A. Suryanto, W. M. Kusumawinahyu, and I. Darti, A Rosenzweig–MacArthur model with continuous threshold harvesting in predator involving fractional derivatives with power law and Mittag–Leffler kernel, *Axioms* **9**, 122 (2020).
- [10] X. Q. P. Wu and L. C. Wang, Analysis of oscillatory patterns of a discrete-time Rosenzweig–MacArthur model, *Int. J. Bifurcation Chaos* **28**, 1850075 (2018).
- [11] F. Munteanu, A study of the Jacobi stability of the Rosenzweig–MacArthur predator-prey system through the KCC geometric theory, *Symmetry* **14**, 1815 (2022).
- [12] M. L. Rosenzweig, Paradox of enrichment: destabilisation of exploitation ecosystems in ecological time, *Science* **171**, 385 (1971).
- [13] A. Hammoum, T. Sari, and K. Yadi, The Rosenzweig–MacArthur graphical criterion for a predator-prey model with variable mortality rate, *Qual. Theory Dyn. Syst.* **22**, 36 (2023).
- [14] A. Chakraborty, M. Singh, D. Lucy, and P. Ridland, Predator–prey model with prey-taxis and diffusion, *Math. Comput. Model.* **46**, 482 (2007).
- [15] E. F. Frølich and U. H. Thygesen, Population games with instantaneous behavior and the Rosenzweig–MacArthur model, *J. Math. Biol.* **85**, 52 (2022).
- [16] H. Cai, A. Ghazaryan, and V. Manukian, Fisher-KPP dynamics in diffusive Rosenzweig–MacArthur and Holling–Tanner models, *Math. Model. Nat. Phenom.* **14**, 404 (2019).
- [17] R. Andrade and C. A. Cobbold, Heterogeneity in behaviour and movement can influence the stability of predator-prey periodic travelling waves, *Bull. Math. Biol.* **85**, 1 (2023).
- [18] V. Weide, M. C. Varriale, and F. M. Hilker, Hydra effect and paradox of enrichment in discrete-time predator-prey models, *Math. Biosci.* **310**, 120 (2019).
- [19] T. Banerjee, P. S. Dutta, A. Zakharova, and E. Scholl, Chimera patterns induced by distance-dependent power-law coupling in ecological networks, *Phys. Rev. E* **94**, 032206 (2016).
- [20] A. Gupta, T. Banerjee, and P. S. Dutta, Increased persistence via asynchrony in oscillating ecological populations with long-range interaction, *Phys. Rev. E* **96**, 042202 (2017).
- [21] P. Hosseini, How localized consumption stabilizes predator-prey systems with finite frequency of mixing, *Am. Nat.* **161**, 567 (2003).
- [22] Y. Zhang and L. Xia, Pattern formation in Rosenzweig–MacArthur model with prey–taxis, *Int. J. Numer. Anal. Model.* **16**, 97 (2018).
- [23] M. A. McPeck, Intraspecific density dependence and a guild of consumers coexisting on one resource, *Ecology* **93**, 2728 (2012).
- [24] D. W. Stephens and J. R. Krebs, *Foraging Theory* (Princeton University Press, Princeton, 1986).
- [25] P. Yodis, *Introduction to Theoretical Ecology* (Harper and Row, NY, 1989).
- [26] B. D. Dalziel, E. Thomann, J. Medlock, and P. De Leenheer, Global analysis of a predator–prey model with variable predator search rate, *J. Math. Biol.* **81**, 159 (2020).
- [27] V. Křivan, Optimal foraging and predator-prey dynamics, *Theor. Popul. Biol.* **49**, 265 (1996).
- [28] V. Křivan and A. Sikder, Optimal foraging and predator-prey dynamics II, *Theor. Popul. Biol.* **55**, 111 (1999).
- [29] V. Křivan and J. Eisner, Optimal foraging and predator-prey dynamics III, *Theor. Popul. Biol.* **63**, 269 (2003).
- [30] P. Gawroński, A. Borzi, and K. Kułakowski, Instability of oscillations in the Rosenzweig–MacArthur model of one consumer and two resources, *Chaos* **32**, 093121 (2022).
- [31] Y.-C. Lai and T. Tél, *Transient Chaos: Complex Dynamics on Finite Time Scales*, Applied Mathematical Sciences Vol. 173 (Springer, New York, 2011).
- [32] O. E. Omel’chenko and T. Tél, Focusing on transient chaos, *J. Phys.: Complex.* **3**, 010201 (2022).
- [33] Z. Hajian-Forooshani and J. Vandermeer, Viewing communities as coupled oscillators: Elementary forms from Lotka and Volterra to Kuramoto, *Theor. Ecol.* **14**, 247 (2021).
- [34] A. P. Møller, Interactions between interactions: predator-prey, parasite-host, and mutualistic interactions, *Ann. NY Acad. Sci.* **1133**, 180 (2008).
- [35] Y. V. Bakhanova, A. O. Kazakov, A. G. Korotkov, T. A. Levanova, and G. V. Osipov, Spiral attractors as the root of a new type of “bursting activity” in the Rosenzweig–MacArthur model, *Eur. Phys. J.: Spec. Top.* **227**, 959 (2018).
- [36] C. S. Holling, Resilience and stability of ecological systems, *Annu. Rev. Ecol. Syst.* **4**, 1 (1973).
- [37] N. R. Smith and B. Meerson, Extinction of oscillating populations, *Phys. Rev. E* **93**, 032109 (2016).
- [38] <https://www.worldwildlife.org/species>.
- [39] J. B. C. Jackson, M. X. Kirby, W. H. Berger, K. A. Bjorndal, L. W. Botsford, B. J. Bourque, R. H. Bradbury, R. Cooke, J. Erlandson, J. A. Estes, T. P. Hughes, S. Kidwell, C. B. Lange, H. S. Lenihan, J. M. Pandolfi, C. H. Peterson, R. S. Steneck, M. J. Tegner, and R. R. Warner, Historical overfishing and the recent collapse of coastal ecosystems, *Science* **293**, 629 (2001).
- [40] C. Kuehn, *Multiple Scale Dynamics*, Applied Mathematical Sciences (Springer, Cham, 2015), Vol. 191.
- [41] H. S. Panigoro, A. Suryanto, W. M. Kusumawinahyu, and I. Darti, Dynamics of an eco-epidemic predator-prey model involving fractional derivatives with power-law and Mittag–Leffler kernel, *Symmetry* **13**, 785 (2021).
- [42] L. Přibylková and L. Berec, Predator interference and stability of predator–prey dynamics, *J. Math. Biol.* **71**, 301 (2015).
- [43] J. Alebraheem, Predator interference in a predator–prey model with mixed functional and numerical responses, *J. M.* **2023**, 4349573 (2023).
- [44] A. Mougi, Predator interference and complexity–stability in food webs, *Sci. Rep.* **12**, 2464 (2022).
- [45] M. E. M. Meza and A. Bhaya, Controlling predator–prey discrete dynamics utilizing a threshold policy with hysteresis, *Appl. Math. Comput.* **217**, 7874 (2011).

- [46] J. Riehl, P. Ramazi, and M. Cao, A survey on the analysis and control of evolutionary matrix games, *Annu. Rev. Control* **45**, 87 (2018).
- [47] P. T. Simin, G. Jafari, M. Ausloos, C. F. Caiafa, F. Caram, A. Sonubi, A. Arcagni, and S. Stefani, Dynamical phase diagrams of a love capacity constrained prey-predator model, *Eur. Phys. J. B* **91**, 43 (2018).
- [48] L. F. Caram, C. F. Caiafa, A. N. Proto, and M. Ausloos, Dynamic peer-to-peer competition, *Physica A* **389**, 2628 (2010).
- [49] N. K. Vitanov, Z. I. Dimitrova, and M. Ausloos, Verhulst-Lotka-Volterra (VLV) model of ideological struggle, *Physica A* **389**, 4970 (2010).
- [50] J. Huisman and F. J. Weissing, Fundamental unpredictability in multispecies competition, *Am. Nat.* **157**, 488 (2001).
- [51] S. Johnson, V. Domínguez-García, L. Donetti, and M. A. Muñoz, Trophic coherence determines food-web stability, *Proc. Natl. Acad. Sci. USA* **111**, 17923 (2014).
- [52] T. Kadoya and K. McCann, Weak interactions and instability cascades, *Sci. Rep.* **5**, 12652 (2015).
- [53] A. Binzer, U. Brose, A. Curtsdotter, A. Eklöf, B. C. Rall, J. O. Riede, and F. de Castro, The susceptibility of species to extinctions in model communities, *Basic Appl. Ecol.* **12**, 590 (2011).